Journal of Scientific & Industrial Research
Vol. 82, May 2023, pp. 529-535
DOI: 10.56042/jsir.v82i05.1087

Hybrid DC-DC Converter with Artificial Intelligence based MPPT Algorithm for FC-EV

B Raja Sekhar Reddy[1]*, V C Veera Reddy[2] & M Vijaya Kumar[1]

[1]Jawaharlal Nehru Technological University, Ananthapuramu 515 002, Andhra Pradesh, India

[2]Sri Padmavati Mahila Visvavidyalayam, Tirupati 517 002, Andhra Pradesh, India

Received 02 June 2022; revised 22 September 2022; accepted 06 October 2022

This manuscript covers the use of a Brushless DC Motor (BLDC) based on a fuel cell in an electric vehicle with a hybrid DC-DC converter with artificial intelligence-based Maximum Power Point (MPP) Tracking. The Boost converter and Cuk converter input stages are integrated in this study to produce a high step-up hybrid boost converter. Only one switch is required in the proposed topology, which decreases voltage stress across the diodes. The converter's overall efficiency increased because the voltage across the switch, diode, and capacitor voltage is less than the output voltage. A new Radial Basis Function Network (RBFN) based MPPT approach is developed for fuel cells based electric vehicles to extract maximum power at ambient temperatures. Computer software programme MATLAB/SIMULINK is used to evaluate the Fuel Cell (FC) fed electric vehicle system.

Keywords: Artificial intelligence, DC-DC converters, Electric vehicle, Fuel cell, MPPT

Introduction

Due to the huge increase in costs for diesel and gasoline, most automobile manufacturers are concerned about pollution and the depletion of fossil fuels and are looking for a substitute for vehicle propulsion. Fuel cells have attracted much interest from automakers because of their high efficiency, high specific energy, minimal noise, and no pollutants.[1] The fuel cell output voltage is affected by water content of the membrane, cell temperature, partial pressure of oxygen, and pressure of hydrogen.[2] Due to the nonlinear voltage-current properties of these fuel cells, only one active point is available for each fuel cell MPPT controllers are necessary in order to maximize the power output of both PV and FC systems, and several methods are covered. The PV and PEMFC systems feed their output voltages through DC-DC boost converters, which raise the voltage. A boost converter is essential for PV and FC systems to increase voltage levels. An inverter is used to direct the output of the DC connection into the grid. This active point offers the highest output voltage and output power under specific operating conditions. Because of its low operating temperature, swift start, and minimal cost, the Proton Exchange Membrane Fuel Cells [PEMFC] were predominantly utilised in vehicles. The PEMFCs only contain water, therefore corrosion is barely noticeable. Additionally, PEMFCs are simple to seal, handle, and assemble since they don't require corrosive fluid in the cell. While fuel processors have been created to enable the use of traditional fuels like natural gas, PEMFCs are particularly well suited for activities utilizing pure hydrogen as fuel.[2,3]

To extract the maximum power from the fuel cell under a variety of operational scenarios, the MPP Tracking (MPPT) approach is required. Some of the MPPT techniques are presented in the literature for monitoring maximum power point. Perturb & Observe [P&O] is the most basic, widely used, straightforward MPPT algorithm. P&O, incremental conductance approaches in the steady state will induce oscillations, decreasing the fuel cell system's efficiency.[4] RBFN efficiently controls the time-varying and nonlinear conditions. In this paper, the maximum power point is calculated using the RBFN. RBFN is effective at time-varying and nonlinear situations.[5,6] Typical Brushless DC motor-driven fuel cell electric vehicle configuration is depicted in Fig. 1. A stack of PEMFC produce output voltage is a low DC output voltage that is unregulated. Due to its limited ability to handle current and its problems with thermal management, a boost converter may not be

*Author for Correspondence
E-mail: rajabayyapureddy@gmail.com

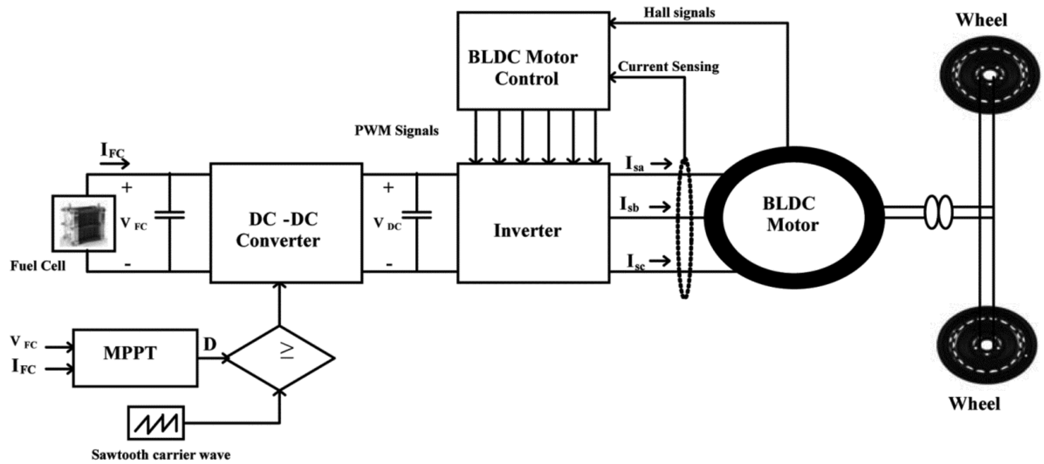

Fig. 1 — Typical brushless DC motor driven fuel cell electric vehicle configuration

suitable for high-power applications. The suggested converter has the benefits like enhanced converter efficiency, increased converter voltage gains, and decreased passive components' size. For low-power fuel cells, a typical DC-DC boost converter (single switch) could be used to increase the output voltage.[7] Various converters, such as interleaved boost converters, quadratic boost, cubic boost, switched inductors, switched capacitors, multi-phase DC-DC converters, and multi-device DC-DC converters, are developed to mitigate these issues.[8–10]

Above MPPT methods produced oscillations, lowering the fuel cell system's efficiency. To overcome these issues, Radial Basis Function Network (RBFN), a neural network approach, is employed to evaluate the MPP. For High-power applications, conventional DC-DC boost converters may not be suitable due to their fewer current handling capabilities and temperature issues. Converters proposed in the literature have the following disadvantages - converter efficiency is low, converter voltage gain is minimum, and the passive components' size is maximum. To mitigate the issues, Novel MPPT Technique and Hybrid DC-DC Converter is Proposed in this Article.

This manuscript proposes a hybrid converter integrating Boost and Cuk Converter to achieve high gain. The proposed converter achieves a high voltage conversion ratio and improved overall efficiency. The problem of leaking inductance is avoided by not using a coupled inductor and all semiconductor devices are subjected to the same low-voltage stress.

For vehicle propulsion, the motor receives the DC voltage. In electric vehicles with fuel cells, the electric motor is critical. The fuel cell's cost and size are greatly reduced when the motor is adequate. In the past, the bulk of automobile manufacturer's DC motors were used in electric vehicle applications. Because of its brushes and commutator, DC motors maintenance cost is high and efficiency is low.[11] The BLDC motors of permanent magnet are commonly utilised in electric vehicle applications due to their ease of control, high reliability, low electromagnetic interference, and great robustness.[12] A fuel cell, ultra-high gain DC-DC converter, VSI, and BLDC motor were all part of the system, and the proposed converter is depicted in Fig. 2. Between the fuel cell and voltage source inverter, the high gain converter serves as a method of communication. To get maximum power out of the fuel cell, an RBFN-based MPPT algorithm is used. The BLDC motor receives power from the high-gain converter through VSI. The electronic commutation of a Brushless DC motor controls the Voltage Source Inverter switches.

Designing of Fuel Cells

Fuel is an energy-conversion electrochemical device. Air and fuel are inputs, and the fuel cell uses a chemical mechanism to turn into water and energy. An individual fuel cell is made up of electrolyte and two electrodes are used to make this device (anode and cathode). The fuel cell does not emit any gases because the reaction only produces heat and water as waste. The PEMFC cell voltage is provided as:[13,14]

$$[V_{FC} = E_{Nernst} - V_{act} - V_{ohm} - V_{conc}] \quad \dots (1)$$

The E_{Nernst} is open-circuit thermodynamic voltage and the E_{Nernst} equation is:

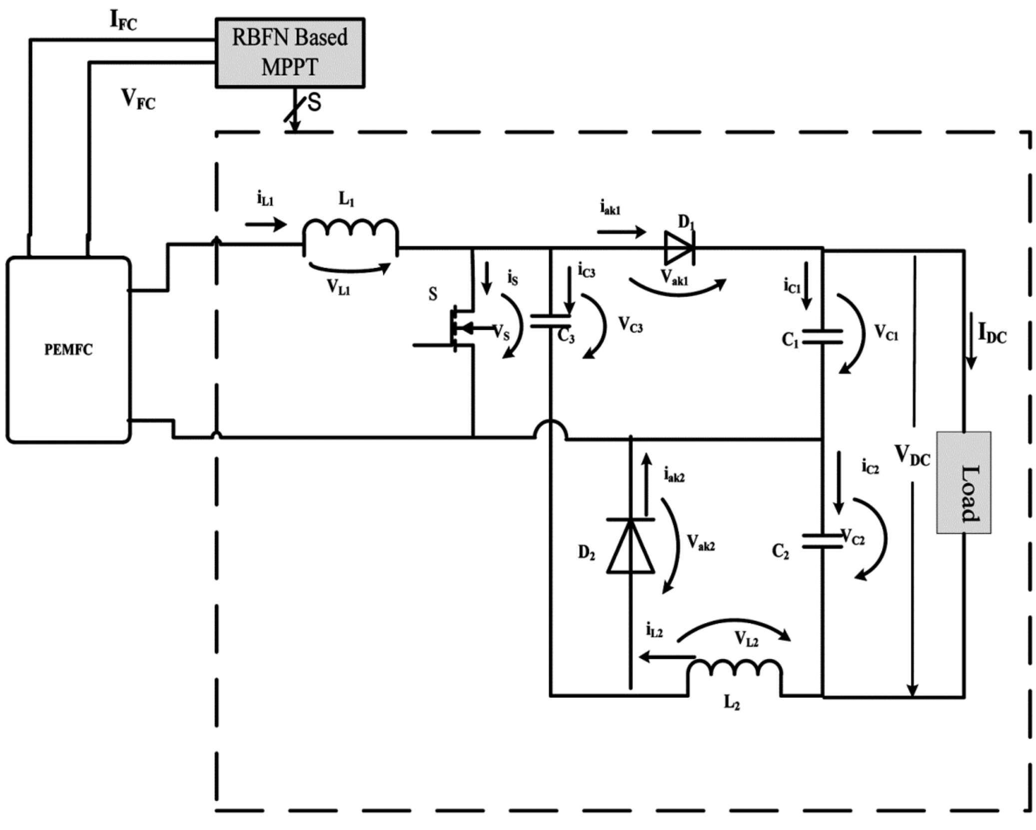

Fig. 2 — Proposed high step-up hybrid boost converter

$$[E_{Nernst} = 1.229 - 8.5 \times 10^{-4}(T - 298.15) + 4.308 \times 10^{-5}\, T(ln(P_{H2}) + 0.5\, ln(P_{O2}))] \quad \ldots (2)$$

Given T stands for absolute temperature (K) and P_{H2} & P_{O2} stand for hydrogen and partial pressure of oxygen (atm). The voltage of activation V_{act} is defined as the sum of anode and cathode activation overvoltage:

$$[V_{act} = -[\delta_1 + \delta_2 T + \delta_3 T\, ln(C_{O2}) + \delta_4 T\, ln(I_{FC})]] \quad \ldots (3)$$

C_{O2}– concentration of dissolved oxygen at the liquid/gas contact

$$[C_{O2} = \frac{P_{O2}}{(5.08\times10^6)\times exp\left(-\frac{498}{T}\right)}] \quad \ldots (4)$$

V_{ohm} – Ohmic overvoltage formulated as

$$[V_{ohm} = I_{FC}\ (R_C + R_M)] \quad \ldots (5)$$

Given R_M stands for equivalent resistance electron flow, R_C stands for resistance of proton, both of which are constant:

$$R_M = \frac{\rho_m L}{A} \quad \ldots (6)$$

'A'- Membrane Active Area in cm^2
'L'-Membrane Thickness in cm,
and'ρ_m'- Membrane Specific Resistivity in Ω-cm

Written as:

$$\rho_m = \frac{181.6[\,1+ 0.03\, J + 0.062\left(\frac{T}{303}\right)^2 (J)2.5]}{[\,G - 0.634 - 3J\,]\, exp[\,4.18\,(1-303T)]} \quad \ldots (7)$$

where, G denotes membrane's water content& J denotes its current density, defined as:

$$J = \frac{I_{FC}}{A} \quad \ldots (8)$$

Following expression can be used to compute the concentration overvoltage.

$$V_{con} = -\frac{RT}{nF} ln\left(1 - \frac{J}{J_{max}}\right) \quad \ldots (9)$$

'R'- Universal gas constant,
'F'- Faraday's constant and
'J_{max}'- Maximum current density.

The PEMFC design specifications are shown in below Table 1.

High Step-up Hybrid Boost Converter (HSHBC)

The proposed converter architecture is shown in Fig. 3. The HSHBC (Table 2) is developed by integrating the boost and cuk converter, and it is analyzed under Continuous Conduction Mode (CCM) and all components are ideal. The following operating modes are outlined as a result of this:

Operating Mode (a) [t_1-t_2]

While the switch S is ON condition the inductors L_1 and L_2 are in charging condition, capacitor C_3 is in discharging mode. The diodes D_1 and D_2 are blocked because of negative voltages Vc_1 and Vc_3.

Operating Mode (b) [t_2-t_3]

In this mode, switch is OFF condition. This mode occurs because of C_3 less than C_1. The inductors L_1 and L_2 energy is decreased and capacitor C_3 is charging mode. D_2 will be turned on and D_1 will be in blocked state.

Table 1 — FC design specifications

Summary	Rating
P_{max} (Max Power)	1.26 kW
V_{max} (Max Voltage)	24.23 V
I_{max} (Maximum Current)	52 A
Total cells	42
Temperature of operation	55°C
Nominal air flow rate	2400

Table 2 — HSHBC parameters

Parameter description	Rating
Switching Frequency- F_s	20 KHZ
Inductor - L_1	2 mH
Inductor - L_2	2 mH
Capacitor – C_1	30 μF
Capacitor – C_2	30 μF
Capacitor-C_3	2 μF

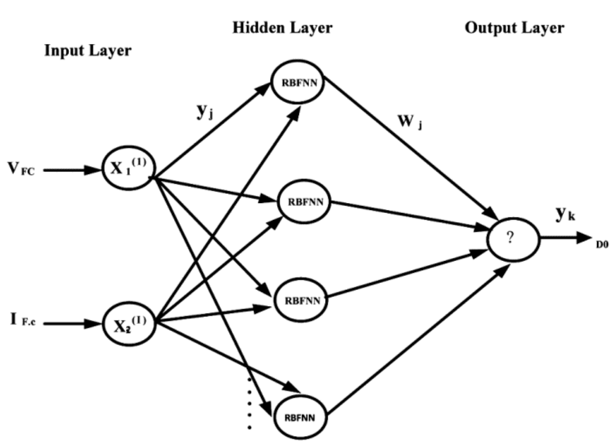

Fig. 3 — RBFN architecture

Operating Mode (c) [t_3-t_4]

In this mode, Switch is OFF state and C_1 voltage is less than or equal to C_3 value. L_1 current will charge C_1 and C_3. Inductors are discharging continuously and diodes are turned off.

The Gain (G) of the proposed converter in CCM

$$\frac{V_0}{V_i} = \frac{1+\delta}{1-\delta} \quad \dots (10)$$

Let $\Delta t_{on} = \delta T$ in Eq. (11); and $\Delta i_{L1} = i_{L1}(t) - i_{L1}(t_0)$

Eq. (12) represents the inductor L_1;

where, V_i - PeakPV output voltage at MPP

$$i_{L_1}(t) = \frac{v_{L_1}}{L}\Delta t_{on} + i_{L_1}(t_o) \quad \dots (11)$$

$$L_1 = \frac{V_i \delta T}{\Delta i_{L_1}} \quad \dots (12)$$

Let $\Delta t_{off} = (1 - \delta)T$.

The inductor L_2 is

$$L_2 = \frac{V_{C_2}(1-\delta)T}{\Delta i_{L_2}} \quad \dots (13)$$

Consider discharge times Δt_1 and Δt_2 as a function of the duty cycle while finding C_1 and C_3.

$$C_1 = \frac{1}{\Delta V_{C_1}}\frac{P_0}{V_o}\Delta t_1 \quad \dots (14)$$

$$C_3 = \frac{1}{\Delta V_{C_3}}\frac{P_0}{V_o}\Delta t_2 \quad \dots (15)$$

Thus, from Eq. (16 & 17) the capacitor C_2 can be obtained.

$$C_2 = \frac{\Delta Q}{\Delta V_{C_2}} \quad \dots (16)$$

$$\Delta Q = \frac{\frac{T}{2}\frac{\Delta i_{L_2}}{2}}{2} \quad \dots (17)$$

$$C_2 = \frac{T\,\Delta i_{L_2}}{8\,\Delta V_{C_2}} \quad \dots (18)$$

Proposed Configuration Control

In the suggested configuration, two control approaches are used. First is for monitoring the fuel cell maximal power, while the other is for BLDC motor operation.

RBFN MPPT Tracking

To extract maximal power for a fuel cell system under diverse temperature settings, MPPT is required. Because of their simple structure and ease of use, the P&O and INC procedures are the most popular MPPT strategies. These strategies may create steady-state oscillations, lowering the fuel cell system efficiency. FLC and neural network techniques are utilized for tracking the MPP more effectively, precisely to overcome the problem.[15] The RBFN MPPT controller is used in the suggested design. The RBFN is a supervised model, and the neural network is an unsupervised feed-forward model. RBFN contains three layers, as shown in Fig. 3 an input (I/P) layer-i, hidden (H) layer-j, and output layer (O/P)-k. In this proposed work, the PEMFC's current and voltage as inputs to the RBFN controller and generate a control signal (D) as output. This information is provided to the proposed high-gain boost converter, which regulates the output voltage.[16,17]

The input layer's nodes are utilized to convey data to the hiding layer. The input layer-i of RBFN input and output are represented as

$$x_i^{(1)}(n) = net_i^{(1)} \quad \dots (19)$$

$$[y_i^{(1)}(n) = f_i^{(1)}[net_i^{(1)}(n)] = net_i^{(1)}(n), i = 1,2] \quad \dots (20)$$

The input layer is x_i^1, hidden layer is$y_i^1$and net_i^1 is the input layer sum. In the middle layery_i^1, every node executes a Gaussian's function. In the RBFN, it is utilised as a membership function.

$$[net_j^{(2)}(n) = -(X - M_j)^T \underset{j}{\Sigma}(X - M_j)] \quad \dots (21)$$

$$[y_j^{(2)}(n) = f_j^{(2)}[net_j^{(2)}(n)]\, exp[\, net_j^{(2)}(n)],\ j = 1,2,\dots..] \quad (22)$$

Given M_j- Gaussian function's mean, j- standard deviation.

The single node (k) output layer generates control signal. (D).

$$[net_k^{(3)} = \underset{j}{\Sigma} w_j y_j^{(2)}] \quad \dots (23)$$

$$[y_k^{(3)} = f_k^{(3)}[net_k^{(3)}(n)] = net_k^{(3)}(n)] \quad \dots (24)$$

'w_j'- the output-to-hidden layer connective weight matrix.

The most widely used MPPT approaches, which benefit from easy implementation and a simple structure. However, these algorithms have oscillations at the maximum power point location at lower irradiance values, which makes it much harder to calculate the maximum power and lowers the efficiency of power transformation.

The RBFNN MPPT algorithm is a universal approximation and quick learning algorithm because it takes use of special activation functions. The RBFN is capable of successful adapting to time-varying conditions. Every time the irradiance changes, the RBFN-based MPPT approach converges to the MPP, reducing power loss. In comparison to other algorithms, the RBFN-based MPPT performs exceptionally well in terms of ripple content, power loss, settling time, and efficiency.

Results & Discussion

The performance of the suggested BLDC motor-fed fuel cell-powered electric vehicle system is evaluated using the simulation results. Consider the following rapid fluctuations in PEMFC temperature as shown in Fig. 4: T = 320 K from 0 to 0.3 sec, T = 310 K from 0.3 to 0.6 sec, and from 0.6 to 0.9 sec T = 330 K.

The output voltage, current, and power wave shapes of a fuel cell from 0 to 0.3 seconds, the fuel cell produces 1080 W, 940 W from 0.3 seconds to 0.6 seconds, and 1240 Watts from 0.6 to 0.9 seconds are also shown in Fig. 5.

The power, voltage and Current at DC Link are depicted in Fig. 6. The recommended RBFN MPPT approach delivers 1060 W, 925 W, and 1230 W at temperatures of 320 Kelvins, 310 Kelvins and 330 Kelvins, respectively.

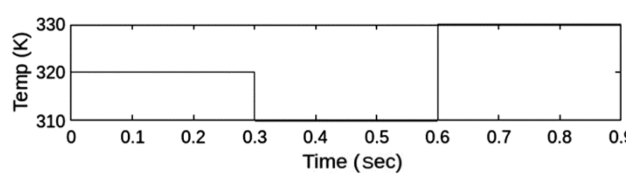

Fig. 4 — Considered variations of temperature in fuel cell system

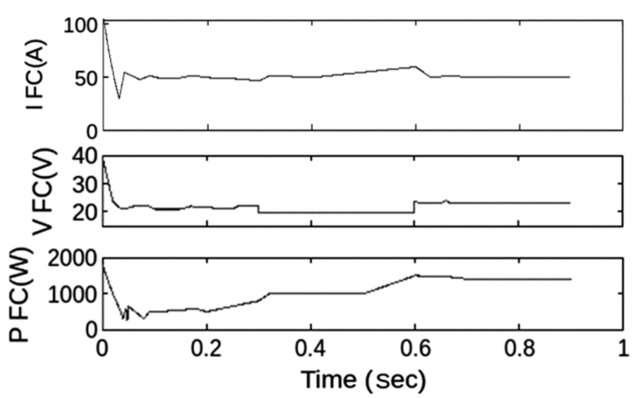

Fig. 5 — PEMFC Power, Voltage and Current at various temperatures

Table 3 — DC link powers Comparison

Parameter	Period (sec)	PEMFC Temperature (˚K)	DC Link Current (Amps)	Voltage (Volts)	Power (Watts)
1.26 kW PEMFC with fuzzy based MPPT	0 to 0.3	320	4.74	215	1006
	0.3 to 0.6	310	4.36	196	844
	0.6 to 0.9	330	5.18	229	1180
1.26 kW PEMFC with RBFN based MPPT	0 to 0.3	320	4.86	224	1060
	0.3 to 0.6	310	4.5	207	925
	0.6 to 0.9	330	5.28	235	1230

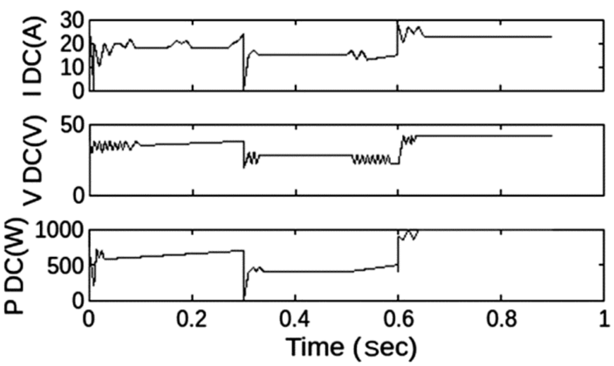

Fig. 6 — Power, voltage and current of DC link at different temperature

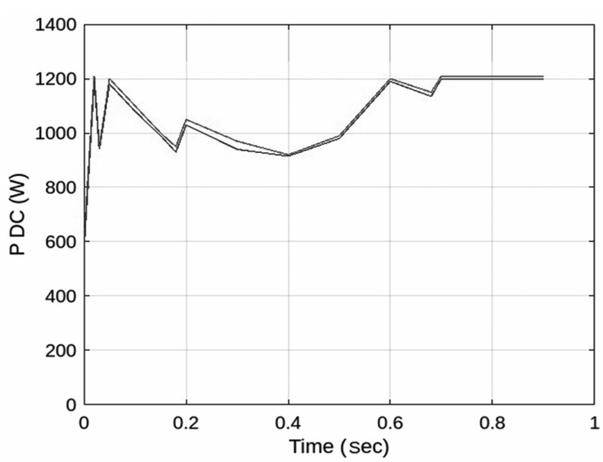

Fig. 7 — DC link powers comparison

The RBFN controller is compared with the fuzzy controller and generates a high o/p power at the DC link, as illustrated in Fig. 7. A comparison of fuzzy and RBFN-based MPPT controllers is shown in Table 3. The proposed Novel MPPT Technique and Hybrid DC-DC Converter was developed for BLDC motor fed fuel cell powered electric vehicle system and simulated. The same BLDC motor fed fuel cell-powered electrical vehicle system was simulated by implementing the fuzzy logic MPPT technique with the load. The simulation results for the two MPPT approaches using the same hybrid converter are compared for the different PEMFC temperatures. From the simulation results, the RBFN-based MPPT Technique with a hybrid converter generates high power at DC link.

Conclusions

The designed BLDC motor-fed fuel cell-powered electric vehicle system is tested with different irradiances by using two different MPPT techniques. The RBFN-based MPPT is implemented for the FC system and compared with fuzzy logic-based MPPT technique. The proposed method can track maximum power with varying solar irradiance conditions. The results from the RBFN MPPT approach show the highest power tracking efficiency of 99.57% when compared to Fuzzy Logic MPPT technique, which has power tracking efficiencies of 99.19%, respectively. Additionally, the controller performs excellently in terms of ripples, power loss, settling time, and efficiency. As a result, compared to the fuzzy logic based MPPT method, the proposed RBFN MPPT method is a practical computational intelligence solution for MPPT applications. The proposed system has shown a variety of desired functionalities, including MPP tracking for the fuel cell, Performance improvement of DC-DC converter, speed control, and BLDC motor soft starting. The second stage involves conducting an experimental test of the proposed converter. The same system can be tested with advanced high-gain DC-DC Converters. Finally, this study provides some recommendations to help the designer choose the best converter topologies in terms of cost, efficiency, and compactness for a specific application.

References

1 Inci M & Trksoy O, Review of fuel cells to grid interface: configurations, technical challenges and trends, *J Clean Prod*, **213** (2019) 1353–1370.

2 Wang M H, Yau H T & Wang T Y, Extension sliding mode controller for maximum power point tracking of hydrogen fuel cells, *Abstr Appl Anal*, **(SI56)** (2013) 1–8, DOI: 10.1155/2013/371064.

3 Reddy R S, Reddy V V C & Kumar M V, A hybrid DC-DC converter with ANFIS-MPPT technique for fuel cell-based electric vehicle, *1st Int Conf Electr Electron Info Commun Technol*, (IEEE) 2022, 1–8, doi: 10.1109/ICEEICT53079.2022.9768499.

4 Esram T & Chapman P L, Comparison of photovoltaic array maximum power point tracking techniques, IEEE *Trans Energy Conv*, **22(2)** (2007) 39–449.

5 Saravana S & Babu N R, Maximum power point tracking algorithms for photovoltaic system–A review, *Renew Sustain Energy Rev* **57**, (2016) 192–204.

6 Ozdemir S, Altin N & Sefa I, Fuzzy logic based MPPT controller for high conversion ratio quadratic boost converter, *Int J Hydrog Energy*, **42(28)** (2017) 17748–17759.

7 Andrade A M S S, Faistel T M K, Guisso R A & Toebe A, Hybrid high voltage gain transformer less DC–DC converter, *IEEE Trans Ind Electron*, **69(3)** (2021) 2470–2479.

8 Zaid M, Khan S, Siddique M D, Sarwar A, Ahmad J, Sarwer Z & A Iqbal, A, Transformer less high gain DC-DC boost converter with reduced voltage stress, *Int Trans Electr Energy Syst* **31(5)** (2021) e12877.

9 Sumathy P, Divya N, Sathik J, Lavanya A, Vijayakumar K, Almakhles D, A comprehensive study on various DC–DC converter voltage-boosting topologies and their applications, *Circuit World*, **48(4)** (2022) 529–549, https://doi.org/10.1108/CW-12-2020-0338.

10 Syrigos S P, Christidis G C, Mouselinos T P & Tatakis E C, A non-isolated DC-DC converter with low voltage stress and high step-down voltage conversion ratio, *IET Pow Electron*, **14(6)** (2021) 1219–1235.

11 Singh B & Kumar R, Solar photovoltaic array fed water pump driven by brushless DC motor using Landsman converter, *IET Renew Pow Gen*, **10(4)** (2016) 474–484.

12 Singh B & Bist V, A BL-CSC converter-fed BLDC motor drive with power factor correction, *IEEE Trans Ind Electron*, **62(1)** (2015) 172–183.

13 Benyahia N, Denoun H, Zaouia M, Rekioua T & Benamrouche N, Power system simulation of fuel cell and super capacitor based electric vehicle using an interleaving technique, *Int J Hydrog Energy*, **40(45)** (2015) 15806–15814.

14 Mebarki N, Rekioua T, Mokrani Z, Rekioua D & Bacha S, PEM fuel cell/battery storage system supplying electric vehicle, *Int J Hydrog Energy*, **41(45)** 20993–21005.

15 Reddy R S, Veera Reddy V C & Kumar M V, Modelling and analysis of DC-DC converters with AI based MPP tracking approaches for grid-tied PV-fuel cell system, *Electr Power Syst Res*, **216** (2023) 109053, ISSN 0378-7796.

16 Rai A K, Kaushika N D, Singh B & Agarwal N, Simulation model of ANN based maximum power point tracking controller for solar PV system, *Sol Energy Mater Sol Cells*, **95(2)** (2011) 773–778.

17 Seshagiri S & Khalil H K, Output feedback control of nonlinear systems using RBF neural networks, *IEEE Trans Neu Netw*, **11(1)** (2007) 69–79.